

All-optical broadcast and multicast technologies based on PPLN waveguide

Lingyun Ye (叶凌云)^{1*}, Ju Wang (王菊)², Hao Hu (胡浩)³,
Jinlong Yu (于晋龙)², and Kaichen Song (宋开臣)¹

¹College of Biomedical Engineering and Instrument Science, Zhejiang University, Hangzhou 310027, China

²School of Electrical and Information Engineering, Tianjin University, Tianjin 300072, China

³DTU Fotonik, Department of Photonics Engineering, Technical University of Denmark, Ørsteds Plads, Building 343, 2800 Kgs. Lyngby, Denmark

*Corresponding author: zjujerry@163.com

Received July 5, 2013; accepted September 16, 2013; posted online November 4, 2013

All-optical 1×4 broadcast and 1×3 multicast experiments of a 40-Gb/s return-to-zero on-off keying (RZ-OOK) signal based on a periodically poled lithium niobate (PPLN) waveguide are demonstrated in this letter. Clear opened eye diagrams and error-free performance are achieved for the broadcast signals at 1541.3, 1543.7, 1548.5, and 1550.9 nm. Multicast technology uses cascaded second-harmonic generation and difference-frequency generation in a Ti:PPLN waveguide. An error-free operation with a negligible power penalty is achieved for the three wavelength-division multiplexing multicast signals at 1533, 1537, and 1541 nm.

OCIS codes: 060.4510, 190.4360.
doi: 10.3788/COL201311.110604.

Photonic networks are currently based on wavelength-division multiplexing (WDM) technologies, and their transmission capacity has been increased to Tbit/s over a single optical fiber. However, packet switching and routing are still performed electronically through optical-electrical-optical conversion^[1]. An all-optical conversion can process signals transparently in data format and data rate, and it potentially consumes low power. All-optical conversions for broadcasting and multicasting are simple, straightforward, and particularly useful for optical switching nodes in WDM systems because of their characteristic of reusing wavelengths^[2–4].

To date, investigations on all-optical broadcasting and multicasting have focused on one of the following mechanisms: four-wave mixing^[5], amplified spontaneous emission (ASE) modulation^[6], and fiber optical parametric amplifier^[7]. Wavelength conversion based on quasi-phase-matched (QPM) nonlinear optical interactions in periodically poled lithium niobate (PPLN) has recently attracted much interest because of its ultrafast response speed^[8]. Wavelength conversions in PPLN waveguides reaching up to 320 Gb/s have been demonstrated^[8]. Compared with wavelength conversion, WDM multicasting or broadcasting can be used to generate data signals for multiple users^[9]. PPLN waveguides have been demonstrated efficiently for optical multicasting/broadcasting using second-order nonlinear effects by quasi-phase matching^[10–12]. PPLN waveguides also offer advantages such as a wide conversion range, an ultrafast response, a high conversion efficiency, and negligible quantum-limited ASE noise^[13–19]. Given these advantages, all-optical broadcasting and multicasting can be achieved by conventional cascaded second-harmonic generation and difference-frequency generation (cSHG/DFG).

In this study, we experimentally demonstrate 1×4 all-optical broadcasting and 1×3 all-optical multicasting of

a 40-Gb/s return-to-zero on-off keying (RZ-OOK) signal by cSHG/DFG in a Ti:PPLN waveguide. In the multicast experiments, the 40-Gb/s RZ-OOK signal is set to the QPM wavelength for second-harmonic generation (SHG) and is sufficiently amplified to generate wavelength-converted signals. All four broadcast signals and three multicast signals are obtained with error-free performance.

A continuous wave (CW, at the wavelength of λ_1) with a data signal (at the wavelength of λ_2) is launched into the PPLN waveguide. If the powers of the CW and the data signal are high, then each signal can act as a pump. As a result, two wavelength-shifted idlers ($\lambda_3 = 2\lambda_1 - \lambda_2$, $\lambda_4 = 2\lambda_2 - \lambda_1$) in the C-band are generated. The new generated signal at the wavelength of λ_3 can also act as a pump and can convert the CW light into another wavelength ($\lambda_5 = 2\lambda_3 - \lambda_1$). Hence, 1×4 multiwavelength broadcast signals will exist at the output of the PPLN waveguide.

The experimental setup for the PPLN-based multiwavelength broadcast of a 40-Gb/s RZ-OOK signal is shown in Fig. 1. The RZ-OOK 40-Gb/s transmitter generates a 40-Gb/s pseudo-random bit sequence (PRBS, $2^7 - 1$) data signal at the wavelength of 1548.5 nm. The 40-Gb/s RZ-OOK signal is amplified by an erbium-doped fiber amplifier (EDFA), filtered by a 1-nm optical band-pass filter (OBF), passed through a 3-dB optical coupler (OC), and launched into a Ti:PPLN waveguide through fiber butt coupling. A CW laser at 1546.1 nm

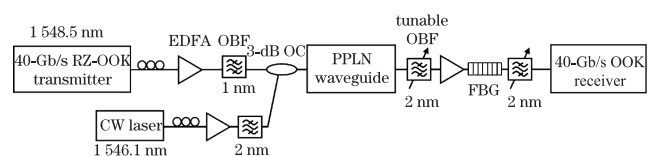


Fig. 1. Experimental setup for the PPLN-based multiwavelength broadcast of a 40-Gb/s RZ-OOK signal.

is amplified, filtered, and launched into the Ti:PPLN through the second input port of the 3-dB OC. The average powers of the data signal and the CW signal at the input of the Ti:PPLN are 25.2 and 25.9 dBm, respectively. The polarization of the data signal is aligned to the transverse magnetic (TM) mode by adjusting the polarization controller (PC). The same procedure is conducted for the CW light. The polarization of the data signal and the CW light is parallel to the optical c -axis of the Ti:PPLN waveguide. A Ti-diffused PPLN waveguide with a $7\text{-}\mu\text{m}$ width and an 80-mm length is used in our experiment. A domain periodicity of $16.4\text{ }\mu\text{m}$ is applied to achieve quasi-phase matching in the C-band ($\sim 1546\text{ nm}$) at elevated temperatures^[6]. The fundamental wavelength is measured as 1546.2 nm with a bandwidth of 0.22 nm. A high-temperature operation ($\sim 180\text{ }^\circ\text{C}$) is conducted to avoid optical-induced damages of the refraction index. The propagation loss of the waveguide is approximately 0.1 dB/cm. The total fiber-to-fiber loss is approximately 6.5 dB, including propagation and coupling losses. At the output of the PPLN waveguide, a filtering subsystem is used to select four broadcast signals with wavelengths at 1541.3, 1543.7, 1548.5, and 1550.9 nm. The center wavelength of the fiber Bragg grating (FBG), which is used to block the high-power CW light, is 1546.1 nm. The broadcast data signals are detected by a 40-Gb/s receiver, which consists of an optical preamplifier and a photodetector. The performances of the broadcast signals are evaluated by an error analyzer.

The optical spectra at the input and output of the PPLN waveguide are shown in Figs. 2(a) and (b), respectively. Several new wavelength-shifted idlers are found at the output of the PPLN waveguides. The broadcast signals are obtained at 1541.3, 1543.7, 1548.5, and 1550.9 nm by tuning the OBFs. The spectra and eye diagrams of the broadcast signals are shown in Fig. 3. The broadcast signal at 1548.5 nm is the original input signal, which is passed through the PPLN waveguide. The noise on “0” levels of the broadcast signals at 1541.3 and 1550.9 nm is extremely small. Nevertheless, the pulses are distorted on “1” levels. By contrast, the noise on “0” levels of the broadcast signal at 1543.7 nm is relatively large, whereas the eye diagram of “1” levels is relatively clear. The clear opened eye diagram indicates the good performance of the four broadcast signals.

The bit error rates (BERs) of the four broadcast signals are measured as a function of the received power, as shown in Fig. 4. The BER curves are plotted for the 40-Gb/s RZ-OOK back-to-back (B2B) signals and the four 40-Gb/s broadcast data signals at 1541.3, 1543.7, 1548.5,

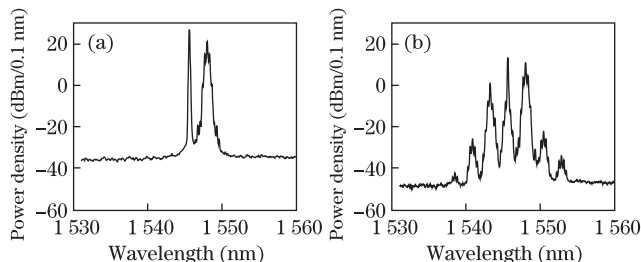


Fig. 2. Optical spectra at the (a) input and (b) output of the Ti:PPLN waveguide.

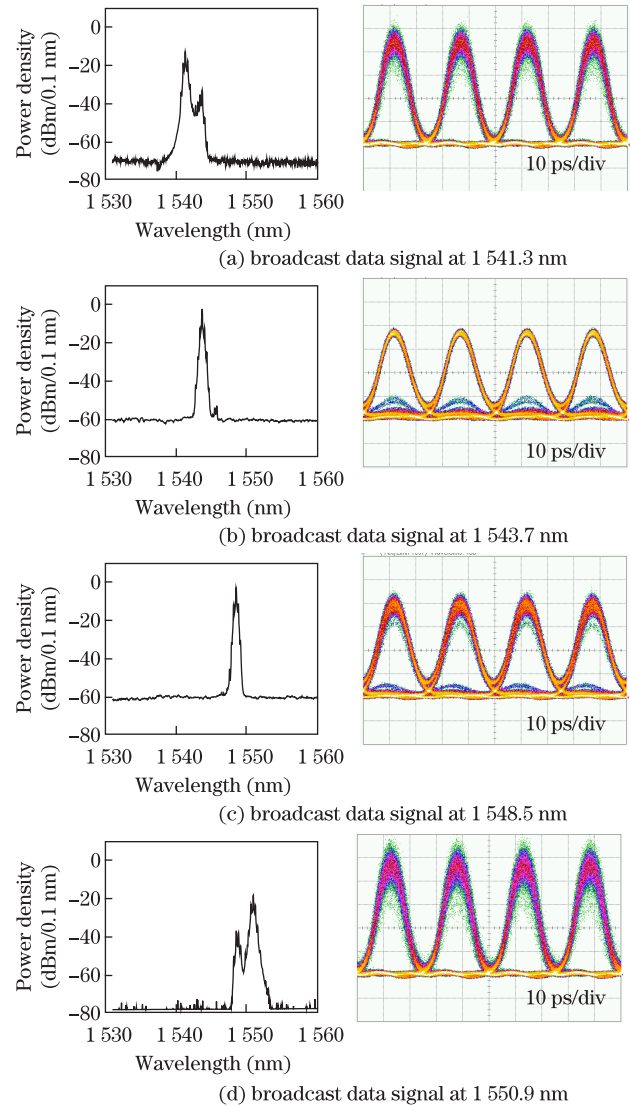


Fig. 3. (Color online) Optical spectra and eye diagrams of the broadcast data signals after filtering the subsystem at (a) 1541.3, (b) 1543.7, (c) 1548.5, and (d) 1550.9 nm.

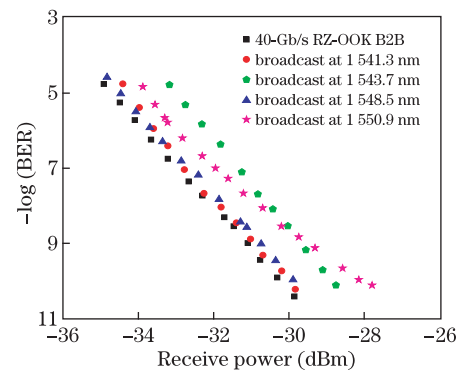


Fig. 4. (Color online) BER curves of the four 40-Gb/s broadcast signals.

and 1550.9 nm. All four broadcast signals exhibit error-free (10^{-9}) performance.

Compared with the B2B case, the power penalties are negligible for the signals at 1541.3 and 1548.5 nm. The maximum power penalty is 2.3 dB for the signal at

1550.9 nm, which is limited by the optical signal-to-noise ratio (OSNR). If the conversion efficiency of the PPLN waveguide is increased or if the coupling loss between the fiber and the waveguide is reduced, then the OSNR of the broadcast signals will be improved.

A 40-Gb/s RZ-OOK data signal (at the wavelength of λ_1) is launched into the PPLN waveguide as a pump, with three CW lights (at wavelengths of λ_2 , λ_3 , and λ_4). The input data signal is set within the QPM wavelength range. This signal acts as the fundamental wave and generates a second harmonic signal (via SHG) at $\sim 0.77 \mu\text{m}$ via quasi-phase matching. Meanwhile, three wavelength-shifted idlers ($2\lambda_1 - \lambda_2$, $2\lambda_1 - \lambda_3$, and $2\lambda_1 - \lambda_4$) are generated via DFG between the second-harmonic signal and the CW lights. The multicast signals at wavelengths of $2\lambda_1 - \lambda_2$, $2\lambda_1 - \lambda_3$, and $2\lambda_1 - \lambda_4$ are at the output of the PPLN waveguide. The wavelength of each multicast signal can be controlled by adjusting that of the corresponding CW light.

The experimental setup for the PPLN-based WDM multicasting of a 40-Gb/s RZ-OOK signal is shown in Fig. 5. Similar to the preceding experiment, a CW light at the wavelength of 1546.1 nm passes through a pulse carver and a Mach-Zehnder modulator, and then generates a 40-Gb/s RZ-OOK data signal (PRBS, $2^7 - 1$). The 40-Gb/s RZ-OOK signal is amplified by an EDFA, filtered by a 1-nm OBF, passed through a 3-dB OC, and launched into a polarization insensitive PPLN subsystem, which has been discussed in detail in Ref. [6]. Three more CW lights at 1551, 1555, and 1559 nm are amplified and launched into the polarization insensitive PPLN subsystem through the 3-dB OC. The average powers of the data signal and the CW signal at the input of the PPLN subsystem are 25.8 and 16.9 dBm, respectively. The powers distributed to the two arms of the polarization beam splitter (PBS) are ensured to be equivalent by adjusting the PC. The polarizations of the three CW lights require no adjustment. At the output of the polarization insensitive PPLN subsystem, three multicast signals (at wavelengths of 1541, 1537, and 1533 nm) are obtained. The multicast data signals are detected by a 40-Gb/s receiver.

The optical spectra at the input and output of the polarization insensitive PPLN subsystem are shown in Figs. 6(a) and (b), respectively. The power of the WDM multicast signals is consistent (the power of each multicast signal is 2.9 dBm), although the polarizations of the three CW lights are not controlled. The multicast signals

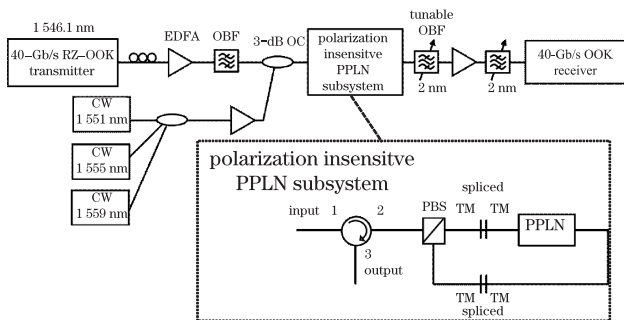


Fig. 5. Experimental setup for the PPLN-based WDM multicasting of a 40-Gb/s RZ-OOK signal.

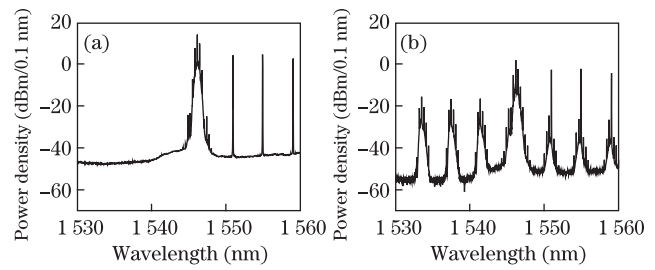
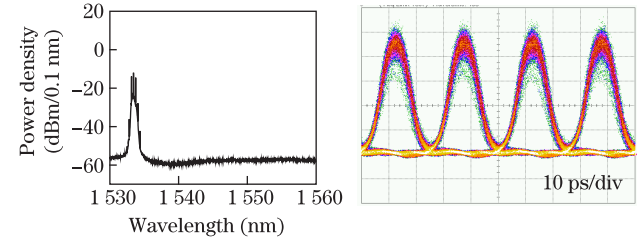
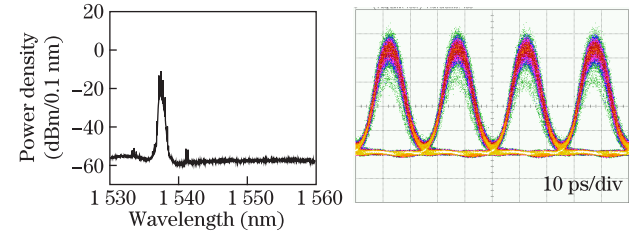


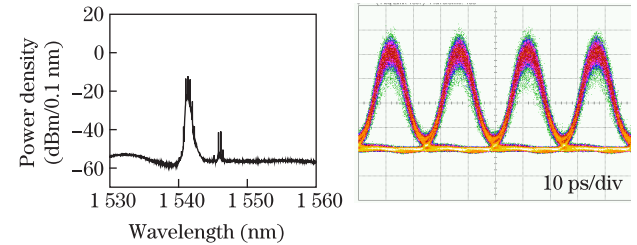
Fig. 6. Optical spectra at the (a) input and (b) end of the PPLN.



(b) multicast signal at 1533 nm



(b) multicast signal at 1537 nm



(c) multicast signal at 1541 nm

Fig. 7. (Color online) Optical spectra and eye diagrams of the WDM multicast signals after filtering at (a) 1533, (b) 1537, and (c) 1541 nm.

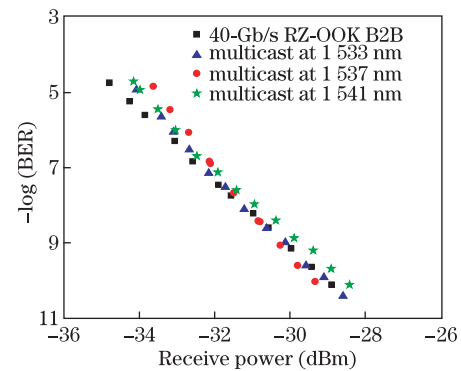


Fig. 8. (Color online) BER curves of the three 40-Gb/s WDM multicast signals.

are obtained at 1533, 1537, and 1541 nm by tuning the OBFs. The spectra and eye diagrams of the WDM multicast signals are shown in Fig. 7. The noise on “0” levels

is extremely small, whereas the noise on “1” levels is relatively large for the three WDM multicast signals. However, the clear opened eye diagram indicates good performance of all WDM multicast signals.

The BER curves of the WDM multicast signals are measured as a function of the received power and are shown in Fig. 8. The BER curves are plotted for the 40-Gb/s RZ-OOK B2B signals and the 40-Gb/s WDM multicast data signals at 1533, 1537, and 1541 nm. All three multicast signals exhibit error-free (10^{-9}) performance. Compared with the B2B case, the power penalties are negligible, and the BER performances are consistent for all multicast signals (<0.5 dB).

In conclusion, we demonstrate the all-optical broadcast and multicast of a 40-Gb/s RZ-OOK signal based on a PPLN waveguide. All 1×4 broadcast signals have clear opened eye diagrams and exhibit error-free performance. The maximum power penalty is 2.3 dB for the broadcast signal at 1550.9 nm, which is limited by the OSNR. The 1×3 multicast technology employs cSHG/DFG in a Ti:PPLN waveguide. An error-free operation with a negligible power penalty is achieved for the three WDM multicast signals at 1533, 1537, and 1541 nm.

The authors would like to thank Dr. Colja Schubert of the Fraunhofer Institute for Telecommunications, Heinrich Hertz Institute for the support in the experiments, and Prof. Wolfgang Sohler for providing the PPLN waveguide.

References

1. W.-D. Zhong and Q. Huang, in *Proceedings of 2010 IEEE International Conference on Communication Systems (ICCS)* 469 (2010).
2. J. Sun, W. Liu, J. Tian, J. R. Kurz, and M. M. Fejer, *IEEE Photon. Technol. Lett.* **15**, 1743 (2003).
3. Z. Zhou, S. Xiao, M. Zhu, and M. Bi, *Chin. Opt. Lett.* **9**, 060602 (2011).
4. L. Liu, M. Zhang, M. Liu, and X. Zhang, *Chin. Opt. Lett.* **10**, 070608 (2012).
5. G. Contestabile, M. Presi, and E. Ciaramella, *IEEE Photon. Technol. Lett.* **16**, 1775 (2004).
6. Y. Shen, J. H. Ng, C. Lu, T. H. Cheng, M. K. Rao, and D. Liu, in *Proceedings of Optical Fiber Communication (OFC) ME1-1* (2001).
7. G. Kalogerakis, M. E. Marhic, and L. G. Kazovsky, *IEEE J. Lightwave Technol.* **23**, 2954 (2005).
8. H. Hu, R. Nouroozi, R. Ludwig, B. Huettl, C. Schmidt-Langhorst, H. Suche, W. Sohler, and C. Schubert, *Appl. Phys. B* **101**, 875 (2010).
9. X. Ma and C. Gan, *Chin. Opt. Lett.* **9**, 040602 (2011).
10. F. Lu, Y. Chen, J. Zhang, W. Lu, X. Chen, and Y. Xia, *Electron. Lett.* **43**, 1446 (2007).
11. M. Gong, Y. Chen, F. Lu, and X. Chen, *Opt. Lett.* **35**, 2672 (2010).
12. M. Ahlawat, A. Bostani, A. Tehranchi, and R. Kashyap, *Opt. Lett.* **38**, 2760 (2013).
13. Y. H. Min, J. H. Lee, Y. L. Lee, W. Grundkoetter, V. Quiring, and W. Sohler, in *Proceedings of Optical Fiber Communication Conference (OFC) FP4* (2003).
14. H. Furukawa, A. Nirmalathas, N. Wada, S. Shinada, H. Tsuboya, and T. Miyazaki, *IEEE Photon. Technol. Lett.* **19**, 384 (2007).
15. H. Hu, R. Nouroozi, R. Ludwig, B. Huettl, C. Schmidt-Langhorst, H. Suche, W. Sohler, and C. Schubert, *J. Lightwave Technol.* **29**, 1092 (2011).
16. J. Wang, J. Sun, X. Zhang, and D. Huang, *J. Lightwave Technol.* **26**, 3137 (2008).
17. A. Bogoni, X. Wu, I. Fazal, and A. Willner, *J. Lightwave Technol.* **27**, 4221 (2009).
18. K. Jo Lee, S. Liu, K. Gallo, P. Petropoulos, and D. J. Richardson, *Opt. Express* **19**, 8327 (2011).
19. H. Hu, R. Nouroozi, W. Wang, J. Yu, H. Suche, and W. Sohler, *IEEE Photon. J.* **4**, 1396 (2012).